

Evaluation of the RF Field Uniformity of a Double-Tuned $^{31}\text{P}/^1\text{H}$ Birdcage RF Coil for Spin-Echo MRI/MRS of the Diabetic Foot

Robert L. Greenman, PhD,^{1*} and Rebecca Rakow-Penner, MS²

Purpose: To evaluate the B1 field uniformity of a double-tuned birdcage coil designed for $^{31}\text{P}/^1\text{H}$ MRI/MRS spin-echo (SE) imaging of the metatarsal head region of the foot in neuropathic diabetic patients.

Materials and Methods: A low-pass double-tuned $^{31}\text{P}/^1\text{H}$ RF birdcage coil was constructed to fit over the adult forefoot. Flip angle (FA) maps were created from B1 data acquired at the 3T ^{31}P (four normal subjects) and ^1H (five normal subjects) frequencies. T2-weighted (T2-W) ^1H images, ^{31}P rapid acquisition with relaxation enhancement (RARE) images, and composite SE pulse CSI data were acquired to demonstrate the uniformity of the resulting images and data.

Results: The means and standard deviations (SDs) of the range of FAs across the feet of the volunteer subjects indicated good uniformity (the maximum coefficients of variation (CVs) for all of the ^{31}P and ^1H FA maps were 7.6% and 7.3%, respectively). The FA values across the metatarsal head region indicated a maximum signal intensity variation of $\pm 3\%$ in a RARE image acquired using an echo train length of 32.

Conclusion: A $^{31}\text{P}/^1\text{H}$ birdcage coil constructed for MRI/MRS studies of the human forefoot provided sufficient signal uniformity of SE data to facilitate accurate ^{31}P concentration measurements in muscle.

Key Words: 3 Tesla; birdcage coil; diabetes; RARE imaging; non-proton MRI

J. Magn. Reson. Imaging 2005;22:427–432.
© 2005 Wiley-Liss, Inc.

IN DIABETES, functional abnormalities of the microvasculature in the distal regions of the lower extremities

result in polyneuropathy, which causes a loss of sensation, vasodilation, and motor function in the muscle (1). These complications have especially profound effects in the feet. Sensory, motor, and autonomic neuropathies in the distal regions of the extremities predispose many diabetics to traumatic insults leading to superficial ulcerations and osteomyelitis (2,3). These pathologies typically occur at the metatarsal head region of the forefoot. The energy metabolism of the muscles in this region may be a measure of the degree of ischemia and the viability of the affected tissues. Thus, a phosphorus-31/proton ($^{31}\text{P}/^1\text{H}$) MRI/MRS examination of the forefoot of diabetic patients could be valuable for assessing the severity of polyneuropathy, monitoring therapeutic intervention, and planning surgical procedures.

Recently introduced spin-echo (SE) methods offer advantages for ^{31}P imaging and spectroscopy. Direct imaging of the ^{31}P metabolites can be accomplished with substantially reduced scan times and improved spatial resolution compared to chemical shift imaging (CSI) MRS techniques using the rapid acquisition with relaxation enhancement (RARE) (4,5) pulse sequence. Also, an SE spectroscopic technique that uses a composite excitation and refocusing pulse to reduce the echo time (TE) has been introduced (6). This technique may have advantages for ^{31}P spectroscopy of human skeletal muscle. The loss of early data points in the free induction decay (FID) of pulse-and-acquire sequences results in reduced SNR and baseline distortion in ^{31}P spectroscopy (7). It is also useful to combine SE ^1H imaging with ^{31}P MRS to acquire SE T2-weighted (T2-W) and proton density (PD)-weighted images (8) for anatomical registration and identification of pathology (2). However, the signal produced by SE sequences is much more susceptible to spatial variations in the pulse flip angle (FA) than FID or gradient-echo sequences. In the case of metabolite concentration measurement, the spatial variations in FA can result in variations in signal intensities, which can lead to errors in concentration measurements (9). In ^1H SE imaging, the FA errors can lead to shading of the image and impact its diagnostic value (9,10).

Several studies have performed lower-extremity MRI/MRS at 0.5T and 1.5T using surface coils. In those stud-

¹Department of Radiology, Beth Israel Deaconess Medical Center and Harvard Medical School, Boston, Massachusetts, USA.

²Department of Radiology, Stanford University, Stanford, California, USA.

Contract grant sponsor: National Institutes of Health; Contract grant number R21 DK58651.

*Address reprint requests to: R.L.G., Department of Radiology, Beth Israel Deaconess Medical Center 330 Brookline Rd., Boston, MA 02115. E-mail: rgreenma@bidmc.harvard.edu

Received 30 November 2004; Accepted 5 May 2005.

DOI 10.1002/jmri.20372

Published online 15 August 2005 in Wiley InterScience (www.interscience.wiley.com).

ies, feet were examined at 0.5T (11) and 1.5T (3), and thigh (12) and calf (8) muscles were examined at 1.5T. The design of a lower-extremity coil for ^1H imaging of the lower thighs and calves at 1.5T using a unique phased array has also been reported (13). Others have used birdcage coils at 1.0 T for ^1H imaging of the calves (8), 1.5T for ^1H imaging of the feet (2), and 3T for ^1H imaging of knees (14). Bus et al (2) and Hajnal et al (8) used a head birdcage coil for this purpose. Suzuki et al (3) used a double-tuned surface coil for a $^{31}\text{P}/^1\text{H}$ examination of the diabetic foot. RF birdcage coils have also been designed to operate efficiently at multiple frequencies, such as ^{31}P and ^1H (15). Although the advantages of the birdcage coil design are well known, this is the first report of a double-tuned $^{31}\text{P}/^1\text{H}$ birdcage coil designed specifically to address problems in the forefoot.

Adiabatic RF pulses have been used to compensate for the nonuniform B1 field of surface coils (16). However, adiabatic RF pulses have a long duration (typically greater than 16 msec), which makes it difficult to achieve short TEs. These pulses are custom designed and are not readily available in pulse sequences supplied by the scanner manufacturers. For a complete MRI/MRS examination using several types of pulse sequences, adiabatic RF pulses must be installed in each sequence that is to be used. A small birdcage RF coil designed to image the metatarsal head region can improve SNR and provide a homogeneous B1 field regardless of the type of pulse sequence employed, obviating the need to install custom-designed adiabatic pulses in each pulse sequence that is to be used.

Performing imaging/spectroscopy of the human foot in a cylindrical RF coil poses some special problems. The location and orientation of the foot within the coil are determined by the anatomy of each individual subject (i.e., size, joint flexibility, wound dressings, etc.). In general, each subject's foot will occupy different regions of the coil, and the axial center line of the foot will often be oriented diagonally in the coil. Additionally, the metatarsal head region of the foot is highly elliptical. It has been hypothesized that nonuniform signal intensity can result when circularly polarized coils, such as the quadrature birdcage design, are used for MRI of elliptical-shaped anatomy (17).

We constructed and evaluated a cylindrical, quadrature, double-tuned $^{31}\text{P}/^1\text{H}$ birdcage coil (15) for imaging the first metatarsal joint of the foot at 3T. We measured the FA distribution that results in this region of the foot when this coil is used for ^{31}P and ^1H imaging and spectroscopy. The results demonstrate that this coil produces a highly homogeneous B1 field across the metatarsal head region of the foot and facilitates the acquisition of uniform-intensity SE MRI and MRS data and metabolite concentration measurements.

MATERIALS AND METHODS

A cylindrical low-pass quadrature RF birdcage coil was constructed and double tuned (15) for the ^{31}P and ^1H resonant frequencies at 3T (51.7 MHz and 127.7 MHz, respectively). The coil consisted of eight struts and had a diameter of 12 cm and a length of 12 cm. A 6-inch length of 4-inch-diameter polyvinyl chloride (PVC) pipe

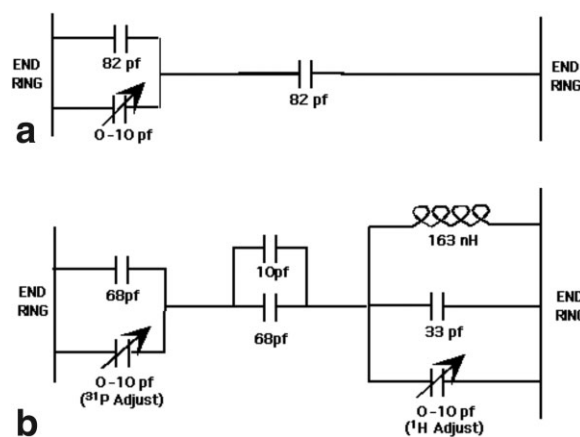


Figure 1. Schematic diagrams of one of the eight struts in the single-tuned version of the birdcage foot coil (a), and one of the eight struts of the double-tuned version of the birdcage coil (b). In both cases, all eight struts were identical.

was used to structurally support the struts and end rings of the coil. The coil was initially single-tuned to 51.7 MHz by the placement of fixed capacitors (American Technical Ceramics, Huntington Station, NY, USA) in series with each of the eight struts. Variable capacitors (0–10 pf) were used for final frequency adjustments (Voltronics Corp., Denville, NJ, USA) (Fig. 1a). Parallel resonant circuits (tank circuits) were then placed into the struts in series with the capacitors that were inserted to tune the coil to 51.7 MHz (Fig. 1b). The values of the original series capacitors and the capacitors in the tank circuit were iteratively adjusted so that the series capacitance and the combined strut and tank circuit inductances resonated at 51.7 MHz, while the strut inductance and the combined series and tank circuit capacitances resonated at 127.7 MHz (15). The final component values for both the single-tuned ^{31}P and the double-tuned $^{31}\text{P}/^1\text{H}$ versions of the birdcage coil are shown in Fig. 1. While other methods exist for double-tuning birdcage coils (18,19), we chose this design for its simplicity and ease of construction. It allows the use of as many struts as necessary to achieve the desired B1 field homogeneity without requiring an unnecessary redundancy of the coil elements. The input impedance of each quadrature drive input was matched to the 50-ohm impedance of the transmission lines with the use of non-resonant inductive loops. Although capacitive matching to the transmission lines is straightforward, inductive matching has the advantage of being relatively insensitive to changes in coil loading (18). In our experience, non-resonant inductive loops provide good coupling efficiency and do not cause splitting of resonant peaks.

All of the MR data acquisitions were performed on a GE 3T whole-body MR scanner (General Electric Medical Systems, Milwaukee, WI, USA). The study protocol was approved by the local institutional review board, and all of the subjects provided written and verbal informed consent prior to the examination. The subjects were placed on the scanning bed in the supine position with their knees elevated by approximately 30 cm using a foam cushion. One foot was placed into the birdcage

radiofrequency (RF) coil so that the metatarsal heads were at the center of the coil.

FA distribution maps were generated from data that were acquired from the feet of normal volunteer subjects by means of a method that was developed for B1 field mapping (20). This method is based on the signal produced by an SE sequence being proportional to $\sin^3(\theta)$, where θ is the FA of the excitation pulse. This is strictly true only when T1 relaxation is complete, but can be approximated when relaxation is nearly complete. The scan TR values were chosen to be about three times the tissue T1 values (95% complete T1 relaxation). SE imaging was performed at the 3T frequencies of ³¹P (repetition time (TR) = 12 seconds, TE = 7.2 msec, number of signal averages (NEX) = 8, field of view (FOV) = 24 cm, slice thickness = 25 mm, and matrix size = 32², scan time = 54 minutes) and ¹H (TR = 7.5 seconds, TE = 7.0 msec, NEX = 1, FOV = 15 cm, slice thickness = 10 mm, matrix size = 128², and scan time = 16 minutes 8 seconds). The data for the FA distribution maps were acquired in the axial plane at the metatarsal head region of the foot. First, the RF input power to the birdcage coil was adjusted for maximum signal across the anatomy of interest within the coil using the scanner's manual calibration function (prescan). This resulted in average excitation/refocusing pulse FAs of 90°/180° across the anatomy. Two SE acquisitions were then performed with the FAs adjusted to 60°/120° for the first acquisition and 120°/240° for the second acquisition. Phosphorus-31 B1 data for FA mapping were acquired from four subjects, and ¹H data were acquired from five subjects. The B1 mapping protocol was repeated four times on different days on one of the subjects at each frequency to assess the repeatability of the B1 field homogeneity and the resulting FA distribution.

Maps of the distribution of FAs across the anatomy being imaged were calculated from the ratio, *r*, of the signal intensity of the two SE data sets (20). The FA in any pixel is (20)

$$FA = \arccos\left(\frac{1}{2 \times r^{(1/3)}}\right) \times 1.5 \quad (1)$$

when the SE images are acquired with excitation/refocusing pulse FAs of 60°/120° in one data acquisition and 120°/240° in the other. The 1.5 factor of Eq. [1] scales the excitation FA values from the 60° nominal value that is applied in the first scan to a 90° nominal FA (20).

SE imaging was performed on the foot of one subject to demonstrate the image quality that results from the use of the dual-tuned birdcage coil. T2-weighted (T2-W) ¹H SE imaging was performed to acquire detailed images of the anatomy (TR = 1.5 s, TE = 30 msec, FOV = 15 cm, matrix = 256 × 256, slice thickness = 2.5 mm, scan time = 6 minutes 24 seconds). Axial ³¹P images were acquired using a RARE pulse sequence (GE fast SE (FSE), two echo trains, 32 echoes per echo train, receiver bandwidth = 4 KHz, TR = 12 s, FOV = 30 cm, matrix = 64 × 64, slice thickness = 25 mm, 10 signal averages, scan time = 4 min, voxel volume = 0.55 cm³)

Table 1
Flip Angle Map Data

Subject	Mean flip angle (degrees)	Flip angle standard deviation (degrees)	Coefficient of variation (CV) (%)
P:A1	97.1	2.9	3.0
P:A2	93.1	3.9	4.2
P:A3	87.8	6.7	7.6
P:A4	91.6	5.7	6.2
P:B	89.6	5.1	5.7
P:C	83.9	3.0	3.6
P:D	89.6	6.6	7.3
H:A1	92.8	4.3	4.6
H:A2	92.8	4.3	4.6
H:A3	92.4	4.5	4.9
H:A4	77.7	3.8	4.9
H:B	91.0	6.6	7.3
H:C	91.8	4.5	4.9
H:D	89.4	6.0	6.7
H:E	75.2	4.5	6.0

while the coil was still single tuned and again after the coil was double-tuned. SNR measurements were performed on the RARE images acquired from the single- and double-tuned versions of the coil to measure the loss in SNR efficiency once the coil was double tuned. CSI data were acquired using an SE pulse sequence that used a composite SE pulse (TR = 3 seconds, SE pulse-pair FA = 60°, FOV = 15 cm, matrix = 16 × 16, bandwidth = 5 kHz, slice thickness = 25 mm, two signal averages, scan time = 25 minutes 36 seconds, voxel volume = 2.34 cm³) (6).

RESULTS

The SNR of the ³¹P in vivo foot image acquired while the birdcage coil was single-tuned was 16.8, while the SNR measured at the same location in the ³¹P image of the foot of the same normal subject acquired using the double-tuned version of the coil was 15.6. The ³¹P SNR of the double-tuned coil was 93% of that of the single-tuned coil.

Table 1 lists the mean, standard deviation (SD), and coefficient of variation (CV) of the FAs calculated across the foot of each subject (P:A-D) at the 3T ³¹P frequency and for each subject (H:A-E) at the 3T ¹H frequency. Rows P:A1-4 and H:A1-4 contain the data that resulted from repeating the FA mapping data acquisitions on the same subjects (P:A and H:A) on four separate occasions. The remaining rows contain the FA information for the remainder of the subjects (P:B-D and H:B-E). The largest CV for the ³¹P FA maps was 7.6%, and the largest CV for the ¹H maps was 7.3%. The variation in the mean values of the FAs is likely due to differences in the manual adjustment of the RF power input to the coil.

FA maps acquired in the axial plane at the metatarsal head region of the foot at the center of the dual-tuned ³¹P/¹H birdcage coil and FA map histograms are shown in Fig. 2. Figure 2a shows a ³¹P FA map, and Fig. 2b shows a ¹H FA map. The scale on the right side of each

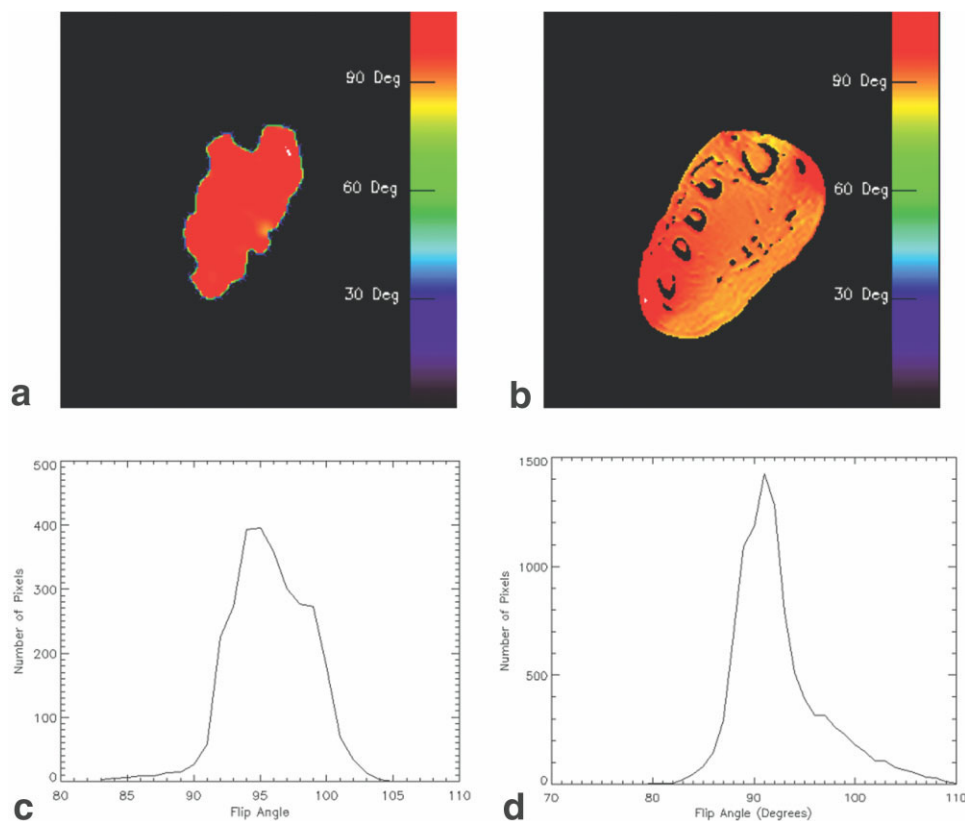


Figure 2. The distribution of FAs in an axial slice located at the center of the dual-tuned birdcage coil. Maps of the range of FAs across the metatarsal head region of the foot at the (a) 3T ^{31}P (51.7 MHz) and (b) ^1H (127.7 MHz) frequencies are shown. c: Histogram of a. d: Histogram of b.

FA map associates a color with FAs ranging from 0° to 110° . Figure 2c and d are histograms of the FA maps in Fig. 2a and b, respectively. The histograms indicate that most of the FAs across the anatomy are within $\pm 10^\circ$ of the central peak. According to Ref. 9, using a RARE sequence with an echo train length of 32 (as used for the RARE image acquisition in this work), this corresponds to a variation in signal intensity of $\pm 3\%$.

A CSI data set obtained using the composite SE pulse sequence is shown in Fig. 3. The PCr peak heights (largest peaks in muscle anatomy) are very uniform in the voxels that contain mostly muscle. The PCr peaks are lower in voxels that contain a combination of muscle and fat or connective tissue.

Figure 4 compares the three types of SE scans that were performed during an examination of one subject. Figure 4a is a ^1H T2-W SE image, b is a ^{31}P RARE image, and c is a PCr image that was generated from the composite SE CSI pulse sequence by integrating the area under the PCr spectral peak in each voxel.

DISCUSSION

A $^{31}\text{P}/^1\text{H}$ MRI/MRS study of the lower extremities, specifically focused on the first metatarsal joint, can provide information about the deep-lying muscle tissue of the diabetic foot (2,3). This information can supplement the information obtained using standard clinical tests (1). We constructed a double-tuned $^{31}\text{P}/^1\text{H}$ birdcage

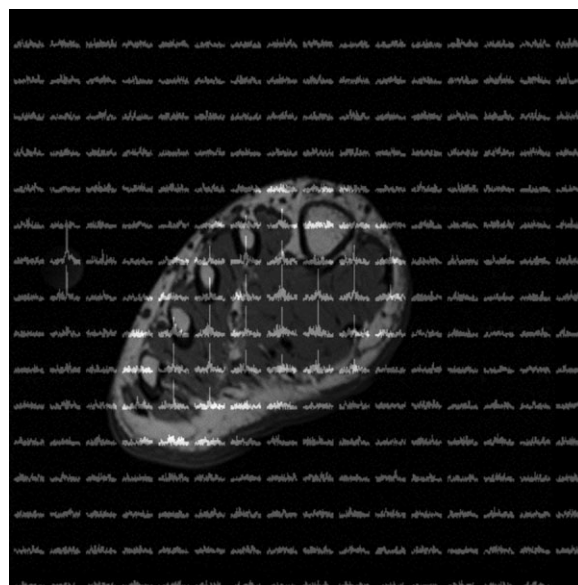


Figure 3. A CSI data set acquired using a pulse sequence with a composite SE pulse. The CSI data are registered to a T2-W ^1H SE axial image using a fiduciary marker (220 mM solution of inorganic phosphate) attached to the birdcage coil (left of foot anatomy in image). The spectral peak heights are uniform across the anatomy and reference standard except in the edge voxels, where partial volume effects are present.

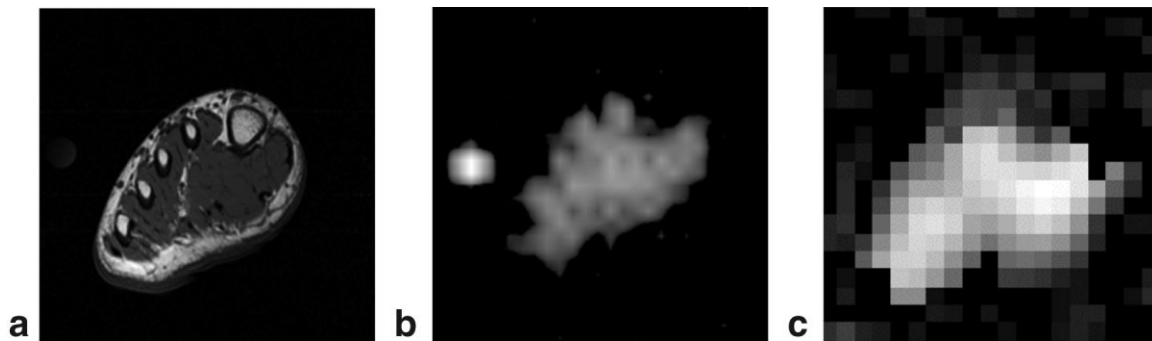


Figure 4. Axial views of the foot acquired through the metatarsal head region in one normal subject: (a) T2-W ^1H SE image, (b) ^{31}P RARE image, and (c) PCr CSI image created by integrating the areas of the PCr peaks in the composite SE CSI data set shown in Fig. 2 after zero-filling to create a 32×32 matrix data set. The circular object to the left of the anatomical data in a and b is the 220 mM inorganic phosphate reference standard.

coil for an MRI/MRS study of the forefoot of diabetic patients at 3T. We then generated FA distribution maps at the ^{31}P and ^1H frequencies that demonstrate a high degree of B1 homogeneity, and acquired ^1H T2-W SE images, ^{31}P RARE images, and ^{31}P composite SE pulse-pair CSI data using this coil.

Some institutions have access to custom-designed adiabatic pulses. However, other institutions have the ability to construct a double-tuned birdcage coil on-site, and there now exist a large number of third-party RF coil vendors. Generally, adiabatic pulses must be custom designed for each pulse sequence. In addition, there are often applications for which the long duration of adiabatic pulses is not acceptable. Once a highly homogeneous volume coil is constructed for imaging/spectroscopy of a given anatomy, any pulse sequence can be used, depending on the goal of the investigation.

The concentrations of the ^{31}P metabolites can be calculated from MRS data using the signal amplitudes of a reference standard of known concentration and a voxel that contains the tissue of interest. Measurement of the absolute ^{31}P concentrations from RARE image intensities has also been demonstrated (9). Substantial spatial variations in the B1 field and the receive sensitivity of the RF coil make these measurements more difficult to obtain and more prone to errors. The FA distribution across the metatarsal head region using the $^{31}\text{P}/^1\text{H}$ birdcage coil constructed for this work will result in a variation of $\pm 3\%$ in signal intensity for a RARE image acquired using a train of 32 echoes (9). In most previously published reports of unlocalized ^{31}P metabolite concentration measurements in normal muscle, the SD values of the PCr concentration ranged from 8% to 15% of the mean value (9). Errors in concentration calculations will be directly proportional to variations in image/localized spectra signal intensity that are due to variations in FA uniformity. The 3% variation in signal intensity demonstrated here is well within the range of variation found in previous ^{31}P concentration measurement studies (9). Therefore, one can obtain sufficiently accurate concentration measurements using this birdcage coil without having to make corrections based on the local B1 field or FA variations. On the basis of these results, we believe that RF field mapping for the purpose of signal-intensity correction is not a necessary

component of an MRI/MRS examination protocol for diabetic patients.

The long T1 relaxation times of phosphocreatine (PCr) and inorganic phosphate (Pi) necessitate the use of long data acquisition times. The RARE pulse sequence, which has the ability to acquire multiple data points after a single excitation, can substantially reduce acquisition times. However, the signal produced by SE and RARE sequences varies as a complex combination of trigonometric functions of the excitation and refocusing FAs raised to various powers, depending on the number of refocusing echoes that are used (9,10). The signal produced by these sequences is therefore highly dependent on variations in the FA of the refocusing pulses. The high B1 field homogeneity afforded by the double-tuned birdcage coil described here minimizes FA variations across the metatarsal head anatomy.

Figure 4b and c show a total ^{31}P RARE image and a PCr CSI image, respectively. While the total ^{31}P image has limited clinical value, the RARE sequence has been used to acquire pure PCr and Pi images with spectrally selective excitation (5). The absolute concentration values of PCr and Pi, as well as the Pi/PCr ratio, can be used to identify ischemic muscle and differentiate viable from unviable tissue (8). A $^{31}\text{P}/^1\text{H}$ MRI/MRS examination may allow the early detection of ischemia and muscle atrophy, and aid in the planning of interventional strategies and monitoring of therapies.

The large spatial variations in the B1 field produced by surface coils result in large spatial variations in the image signal intensity of SE acquisitions. We have demonstrated that a very uniform FA can be achieved across the metatarsal head region of the foot despite its elliptical shape and unpredictable orientation within a double-tuned birdcage RF coil. A larger double-tuned birdcage coil would allow a $^{31}\text{P}/^1\text{H}$ examination of anatomy ranging from the toes to the knee. Such a coil design could be used in an examination to assess peripheral vascular disease as well as the complications associated with diabetes. The use of double-tuned birdcage RF coils can improve the quality of MRI/MRS examinations of the lower extremities.

REFERENCES

1. Britland S, Young R, Sharma A, et al. Relationship of endoneurial capillary abnormalities to type and severity of diabetic polyneuropathy. *Diabetes* 1990;39:909-913.
2. Bus SA, Yang QX, Wang JH, et al. Intrinsic muscle atrophy and toe deformity in the diabetic neuropathic foot: a magnetic resonance imaging study. *Diabetes Care* 2002;25:1444-1450.
3. Suzuki E, Kashiwaga A, Hidaka H, et al. 1H and 31P-magnetic resonance spectroscopy and imaging as a new diagnostic tool to evaluate neuropathic foot ulcers in type II diabetes. *Diabetologia* 2000;43:165-172.
4. Greenman RL, Elliott MA, Vandeborne K, et al. Fast imaging of phosphocreatine using a RARE pulse sequence. *Magn Reson Med* 1998;39:851-854.
5. Greenman RL, Axel L, Ferrari V, et al. Fast imaging of phosphocreatine in the normal human myocardium using a three-dimensional RARE pulse sequence at 4 Tesla. *J Magn Reson Imaging* 2002;15:467-472.
6. Lim K, Pauly J, Webb P, et al. Short TE phosphorus spectroscopy using a spin-echo pulse. *Magn Reson Med* 1994;32:98-103.
7. Brown TR, Kincaid BM, Ugurbil K. NMR chemical shift imaging in three dimensions. *Proc Natl Acad Sci U S A* 1982;79:3523-3526.
8. Hajnal JV, Roberts I, Wilson J, et al. Effect of profound ischaemia on human muscle: MRI, phosphorus MRS and near-infrared studies. *NMR Biomed* 1996;9:305-314.
9. Greenman RL. Quantification of the 31P metabolite concentration in human skeletal muscle from RARE signal intensity. *Magn Reson Med* 2004;52:1036-1042.
10. Greenman RL, Shirosky J, Mulkern R, et al. Double inversion black-blood fast spin-echo imaging of the human heart: a comparison between 1.5T and 3.0T. *J Magn Reson Imaging* 2003;17:648-655.
11. Brash P, Fostert J, Vennart W, et al. Magnetic resonance imaging techniques demonstrate soft tissue damage in the diabetic foot. *Diabet Med* 1999;16:55-61.
12. Choe B-Y, Jee W-H, Suh T-S, et al. Evaluation of the effects of high dose irradiation on canine thigh muscle by follow-up magnetic resonance imaging and phosphorus-31 magnetic resonance spectroscopy. *Invest Radiol* 1998;35:300-307.
13. Brown R, Mareyam A, Reid E, et al. Novel RF coil geometry for lower extremity imaging. *Magn Reson Med* 2004;51:635-639.
14. Peterson D, Carruthers C, Wolverson K, et al. Application of a birdcage coil at 3 Tesla to imaging of the human knee using MRI. *Magn Reson Med* 1999;43:215-221.
15. Isaac G, Schnall M, Lenkinski R, et al. A design for a double-tuned birdcage coil for use in an integrated MRI/MRS examination. *J Magn Reson* 1990;89:41-50.
16. Garwood M, Ugurbil K. B1 insensitive adiabatic RF pulses. In: Bronskill M, Sprawls P, editors. *The Physics of MRI-1992 AAPM Summer School Proceedings*. Woodbury, NY: American Institute of Physics, Inc.; 1993. p 110-147.
17. Sled J, Pike B. Standing-wave and RF penetration artifacts caused by elliptical geometry: an electrodynamic analysis of MRI. *IEEE Trans Med Imaging* 1998;17:653-662.
18. Matson G, Vermathen P, Hill T. A practical double-tuned 1H/31P quadrature birdcage headcoil optimized for 31P operation. *Magn Reson Med* 1999;42:173-182.
19. Murphy-Boesch J, Srinivasan R, Carvajal L, et al. Two configurations of the four-ring birdcage coil for 1H imaging and 1H-decoupled 31P spectroscopy of the human head. *J Magn Reson B* 1994;103:103-114.
20. Insko E, Bolinger L. Mapping of the radio frequency field. *J Magn Reson* 1993;103:82-85.